Application of color infrared aerial photography to assess macroalgal distribution in an eutrophic estuary, Upper Newport Bay, California

Nikolay P. Nezlin, Krista Kamer[1] and Eric D. Stein

Abstract

Newport Bay is a large estuary in southern California that is subject to anthropogenic nutrient loading, eutrophication, and hypoxia. Ground-based methods of assessing algal extent for monitoring and management are limited in that they cannot provide a synoptic view of algal distribution over comparatively large areas. The goal of this study was to explore the application of color infrared aerial photography as an alternative for analyzing the changes in the abundance of exposed macroalgae. Three surveys combining remote sensing (color infrared aerial photography) and ground-based sampling to quantify macroalgal mat coverage were carried out in Upper Newport Bay (UNB) between July and October 2005. Airborne photographs (scale 1:6000) collected during daytime low tides, clear skies and appropriate sun angle were digitized to 25 cm resolution, orthorectified, georegistered and combined into three mosaic composite digital images: one for each survey. During each aerial photography survey, macroalgal percent cover was measured on the ground by the point-intercept method in a 6.25 m^2 area at ~30 locations distributed along the water's edge throughout the intertidal mudflat area. There were three main types of cover: *Ulva* spp. (green algae), *Ceramium* spp. (red algae), and bare surface (mud and mussel beds). To analyze similarities between spectral signatures in the images and cover types, the pixels corresponding to the ground samples from each survey were grouped into clusters based on similarity of their spectral signatures. To establish relationships between spectral signatures in the images and cover as determined from ground data, pixels in each composite image corresponding to ground samples from the same day that were characterized by >90% of one cover type were attributed to that cover type. Ground samples comprised of a mixture of cover types were used for accuracy assessment. Before classification, each digital image was transformed by the Minimum Noise Fraction Rotation method to remove noise and enhance contrast between the classes. For classification of each composite image, the Spectral Angle Mapper scheme was used: all pixels in each image were attributed to the identified classes and the areal extent of each class was estimated. According to these assessments, the macroalgal coverage in UNB increased from 37% in July to 57% in September to 80% in October, and during this time *Ulva* spp. replaced *Ceramium* spp. as the dominant alga. This analysis showed that color infrared aerial photography is an effective tool for assessing estuarine, intertidal macroalgal coverage.

Introduction

Large blooms of opportunistic macroalgae such as *Ulva* spp. occur in estuaries and coastal lagoons throughout the world (Sfriso *et al.* 1987, 1992; Schramm and Nienhuis 1996; Raffaelli *et al.* 1999) often in response to increased nutrient loads from developed watersheds (Valiela *et al.* 1992, Nixon 1995, Paerl 1999). While these algae are natural components of estuarine systems and play integral roles in estuarine processes (Pregnall and Rudy 1985, Kwak and Zedler 1997, Boyer 2002), blooms are of ecological concern because they can reduce the habitat quality of an estuary. They can deplete the water column and sediments of oxygen (Sfriso *et al.* 1987, 1992; Peckol and Rivers 1995) leading to changes in species composition, shifts in community structure (Raffaelli *et al.* 1991, Ahern *et al.* 1995, Thiel

[1] *Moss Landing Marine Laboratories, Moss Landing, CA*

and Watling 1998), and loss of ecosystem function.

Methods of assessing macroalgal distribution and abundance often involve ground-based measurements of percent cover or biomass at multiple locations in a system. Data can be extrapolated from the individual measurements to the entire system, but the appropriateness of this relies on the degree to which the sampling locations represent the larger system. These methods are limited in that they cannot provide a synoptic view of algal distribution over comparatively large areas due to the limited number of samples that can be collected and processed during each survey and often insufficient resources to sample the entire study area. In contrast to more stable terrestrial landscapes that can be sampled over longer time periods, this problem is especially crucial in variable marine environments where macroalgae may drift with the tides (Kamer *et al.* 2001) and change location daily.

Remote sensing (i.e., aerial or satellite image analysis) provides an alternative to ground-based methods for assessment of macroalgal extent. Aerial photography provides more appropriate spatial resolution than satellite imagery for assessment of spatial patterns of aquatic vegetation along seashores, including estuaries (Lehmann and Lachavanne 1997). Satellite observations are more cost-effective (Ferguson and Korfmacher 1997), but the spatial resolution of satellite imagery severely limits its possible utilization for aquatic vegetation mapping. Typically, aquatic vegetation forms narrow strips along the edges of water bodies (Kirkman 1996); these strips are barely wider than the highest resolution of most present day satellites (e.g., 20 m for SPOT and 30 m for Landsat ™). The problem is especially pronounced in southern California where estuaries are often small and the intertidal areas are limited to narrow zones or areas within the estuary.

Aerial photography is particularly well suited for quantitative analysis of terrestrial vegetation where it is necessary to discern areas covered by different surface types (Campbell 1987, Avery and Berlin 1992, Wilkie and Finn 1996, Jensen 2000, Lillesand and Kiefer 2000). For this, color infrared (CIR) photography is an effective method, because it emphasizes the contrast between vegetated and non-vegetated surfaces. In contrast to natural color photography representing three main visible color bands (i.e., blue, green, and red), CIR photography transforms green, red, and near-infrared wavebands into blue, green and red, respectively. Vegetation, in contrast to non-vegetated surface, strongly reflects in near-infrared; as such, in CIR imagery different kinds of vegetation are easily distinguishable by red-color areas of different color tone, representing different levels of near-infrared reflectance (Avery and Berlin 1992). Airborne imagery can also be collected using digital cameras and hyperspectral radiometers which provide higher spectral resolution than traditional film photography (Myers and Miller 2005).

In coastal ocean sciences, aerial photography has been used for assessment of various biological parameters (Hilton 1984), including chlorophyll concentration and phytoplankton biomass in coastal waters (Harding *et al.* 1994, Richardson *et al.* 1994, Hoogenboom *et al.* 1998), coastal plume tracers (Carder *et al.* 1993), benthic substrates (Werdell and Roesler 2003, Vahtmae *et al.* 2006), coral reefs (Mumby *et al.* 1998; Andrefouet *et al.* 2003, 2004; Mumby *et al.* 2004), and different kinds of benthic macrophytes including kelp (Jensen *et al.* 1980, Deysher 1993) and seagrass meadows (Bulthuis 1995, Ferguson and Korfmacher 1997, Robbins 1997, Ward *et al.* 1997, Pasqualini *et al.* 1998, Kendrick *et al.* 2000). Past studies have shown that a combination of green, red, and near-infrared wavebands (i.e., CIR) is best for identification of surface macrophytes in freshwater basins (Malthus and George 1997).

To date, only a handful of studies have used aerial photography to identify macroalgae in marine and estuarine habitats. Several studies have focused on deep estuaries or embayments (Bulthuis 1995, Sheppard *et al.* 1995) as opposed to the shallow estuaries that form along much of the Pacific Coast. One exception is the study by Young *et al.* (1998), which successfully used CIR aerial photography to map macroalgae and eelgrass in Yaquina Bay, a shallow estuary in Oregon. Ground truth data were collected for several days before and after the overflights. Classification of aerial imagery was in good agreement with ground data when the density of vegetation exceeded 75% cover. At lower densities of macroalgae, the agreement was lower, indicating that remote sensing methods may be less sensitive to low densities of algae than ground surveys (D. Young, personal communication).

The goal of this study was to explore the application of CIR aerial photography as an alternative to ground-based methods to analyze the changes in the abundance of macroalgae in Upper Newport Bay (UNB), an eutrophic estuary in southern California.

Our specific objectives were to determine if the area in UNB covered by macroalgae could be accurately assessed by aerial CIR photography, to identify the best methods of imagery processing and data transformation, and to compare system-wide estimates of macroalgal extent based on ground measures and aerial photography. We also analyzed spatial and temporal patterns of macroalgal abundance in different parts of the estuary, and discuss the limitations of CIR, the problems we encountered, and priority areas for future research.

Methods

Study Site

UNB (Figure 1) is the second largest estuarine embayment in southern California. The main freshwater inflow is from San Diego Creek, which drains 85% of the 400-km^2 watershed. The main channel of UNB is wide with extensive broad mudflats and shallow areas; the center of the channel is routinely dredged to 5 m below sea level for sediment retention and navigational purposes. UNB is separated from the Pacific Ocean by Lower Newport Bay, which has been dredged and developed into a marina with no natural wetland area remaining. Water residence time in UNB averages one week during neap tide (RMA 2000).

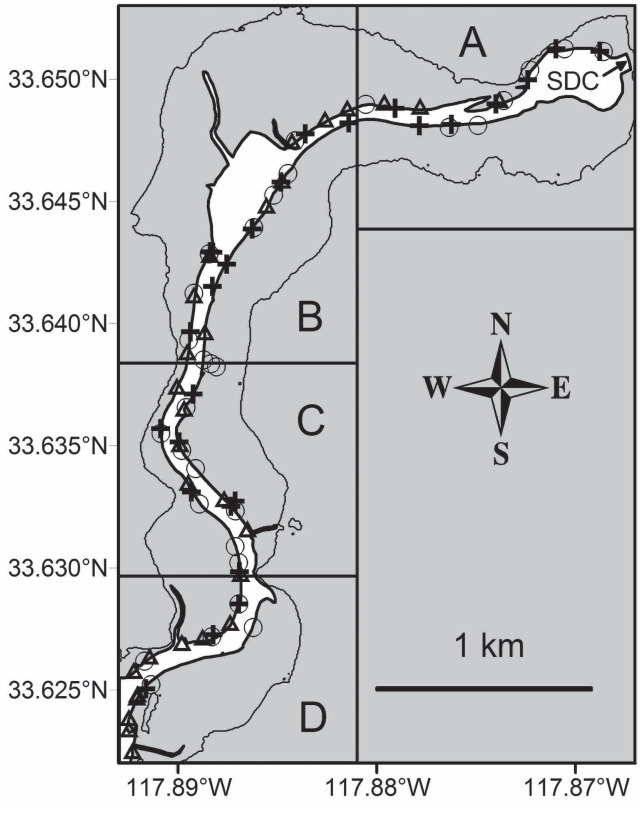

Figure 1. The Upper Newport Bay study area in southern California including four regions (A - D). Thick line indicates water edge, thin line is 32-m DEM level. Land areas are shaded. Triangles, circles and crosses indicate samples collected July 25, September 17, and October 31, 2005, respectively. SDC is the location of San Diego Creek mouth.

UNB is a state ecological reserve and provides critical refuge, forage, and breeding habitat for a number of terrestrial and aquatic threatened and endangered species as well as significant spawning and nursery habitats for commercial and non-commercial fish species. UNB is subject to anthropogenic stressors. Much of the watershed has been converted from orchards and row crop farms to an urban environment. By the late 1980s, 64% of the watershed area was used for residential and commercial purposes (Gerstenberg 1989). Historically, high nutrient loads from the watershed have resulted in macroalgal blooms in UNB (Kamer *et al.* 2001, Kennison *et al.* 2003).

Remote-sensing Data Collection and Analysis

High-resolution CIR aerial photography and ground-based field measurements were used to determine exposed, intertidal macroalgal distribution in UNB three times from July through October 2005. Aerial images were collected during daytime low tides (<0.70 m) with clear skies and sun angle >30° above the horizon on July 25, September 17, and October 31, 2005, by SkyView Aerial Photography, Inc. (San Clemente, CA). Vertical aerial photographs were taken by a forward image-motion compensating GPS-triggered camera with a 153-mm lens. Kodak Aerochrome III Infrared film in 23 x 23 cm format was used. The images were collected from a height of 1000 m resulting in a nominal scale of 1:6000. The frontal overlap between photographs was 60% and side overlap was 40%, in accordance with the recommendations for airborne remote sensing (Myers and Miller 2005). Thirty-three images were collected on July 25, 36 on September 17, and 33 on October 31, 2005. All images were digitized on a high-resolution photogrammetric color scanner at a scanning resolution of 32 microns (800 dpi) in 24 bit color and saved in a TIFF format. The final ground sample distance was 25 cm; an area 10 x 10 pixels was equal to 2.5 x 2.5 m (6.25 m^2). Each digital image contained three wavebands, representing green (500 - 600 nm), red (600 - 750 nm), and near-infrared (750 - 1000 nm).

To provide a data set to interpret the aerial images and assess accuracy, macroalgal abundance was measured on the ground during each overflight. Percent cover of macroalgae was recorded at ca. 30 locations distributed along the water's edge throughout the exposed mudflat area by placing a 1.25 x 1.25 m quadrat strung with two orthogonal sets of five equally spaced taut strings in the four compass sectors around a central point. The cover type (macroalgal species, bare mud, mussels, or other) under each intercept was recorded for a total of 100 points within a 2.5 x 2.5 m (6.25 m^2) area. The location of the central point was recorded with a submeter accuracy GPS. All ground sampling was conducted within the low tide period corresponding with the overflights (approximately five hours) to minimize error associated with drift of the macroalgal mats during inundation. The three basic cover types were identified: *Ulva* spp. (green algae), *Ceramium* spp. (red algae), and bare surface (mud and mussel beds). Previous studies of UNB have reported the occurrence of both *Enteromorpha* and *Ulva* spp. (Kamer *et al.* 2001, Kennison *et al.* 2003). Based on recent genetic studies (Hayden and Waaland 2002, Hayden *et al.* 2003), we have included species formerly referred to as *Enteromorpha* in the genus *Ulva*.

The analysis of UNB imagery included four steps: (1) creation of georegistered composite images for each survey based on geometric transformations (i.e., orthorectification, georegistration and mosaicing); (2) image enhancement achieved by Minimum Noise Fraction Rotation (MNF) transformation; (3) analysis of correspondence between aerial image spectral signatures and corresponding ground-measured cover using K-mean cluster analysis; and (4) estimation of the areas covered by macroalgae in each composite image using Spectral Angle Mapper (SAM) pixel classification method. These steps correspond to the conventional approach used in processing of digital images (e.g., Caloz and Collet 1997). All images were processed using ENVI software Version 4.2 (Research Systems, Inc., Boulder, CO). Each image was orthorectified (i.e., corrected for distortions introduced by the camera geometry, look angles, and topography) and georegistered using the coordinates of recognizable landmarks (25 - 40 for each image). Ground control points (GCPs) along the water's edge were collected during field sampling; other GCPs were obtained from the "Google Earth" website (version 3.0). All images taken during one flight were merged using ENVI mosaic option, creating one composite georegistered image of 0.25-m spatial resolution for each survey.

Next, the areas not relevant to the analysis were removed from each composite image. We clipped the areas in which elevation exceeded 32 m above the image reference level using a high-resolution Digital Elevation Model (DEM) obtained from the National Oceanic and Atmospheric Administration Coastal Services Center/Coastal Remote Sensing (CRS) Program website (http://www.csc.noaa.gov/crs/). This DEM was developed from recent airborne Interferometric Synthetic Aperture Radar (IfSAR) observations and has pixel resolution ranging from 1.25 to 2.50 m. The water surface, the areas of low elevation other than intertidal zone (e.g., slips with recreational boats) and the areas covered by vascular plants (dominated in UNB by *Spartina foliosa* and *Salicornia* spp.) were removed manually by creating a mask. As all ground data used for classification (see below) were collected in the intertidal zone rather than in water or the zone covered by vascular plants, we could not segregate these three zones using image classification methods. We used expert assessment of CIR photographs, where water was clearly distinguished by its dark color and the areas covered by vascular plants by rough texture and sharp edges.

Before classification, images were transformed in order to more clearly separate patterns from random differences in pixel coloration. The goal of this transformation was to remove noise (i.e., differences between image pixels that are not related to differences in vegetation) and make each image more consistent to achieve better classification results. All three composite CIR images (each containing three bands) were transformed by MNF method (Green *et al.* 1988). The MNF method includes two cascaded Principal Components transformations. The first transformation, based on an estimated noise covariance matrix, decorrelates and rescales the noise in the data, resulting in a transformed image in which the noise has unit variance and no band-to-band correlations. The second step is a standard Principal Components transformation of the noise-whitened data. In general, this transformation enables a reduction of the dimensionality of the image spectrum to segregate noise in the data, which makes sense when the number of bands is substantially higher than three, such as in hyperspectral imagery. The analyzed images contained only three bands; as such, the dimensionality of the data was not changed, but

the separability (i.e., the quantitative measure of difference) between the classes and unclassified samples dramatically improved.

Relationships between spectral signatures in the images and cover as determined from ground data were established. To illustrate the similarities and differences between substrates and spectra, clusters of pixels representing identifiable classes of cover for each survey were identified. Typically each 6.25-m^2 ground sample was associated with 99 to 101 25-cm pixels in a corresponding 6.25-m^2 area at the aerial image centered around the coordinates of the center of the ground sample. Pixels corresponding to areas where ground data were collected were grouped into clusters based on similarity of their spectral signatures. This was done using the K-mean clustering method based on Euclidean distances between samples in 3-dimensional space representing 3 wavebands. The criterion of clustering was minimization of variability within clusters and maximization of variability between clusters. For each of these clusters, the mean percent cover of each cover type (*Ulva* spp., *Ceramium* spp., bare surface, other) was estimated by averaging the results of ground samples associated with each cluster. The clusters included both homogenous and mixed cover types, e.g., *Ulva* and *Ceramium* spp.

To assess the exposed intertidal mudflat area covered by each cover type, ground samples with >90% of one cover type (i.e., homogenous) were selected as "training areas" for image classification (Table 1). Pixels in each composite image corresponding to these ground samples were attributed to the respective cover type. All pixels of the MNF-transformed images were processed by the method of supervised classification, i.e., each pixel was compared to training areas and most of them were attributed to distinct classes associated with the training areas. Those pixels that appeared to be different from all training areas were attributed to an "unclassified" group. As a method of supervised classification we used the SAM algorithm. As a measure of similarity between the training area and each pixel, SAM uses the angle between their spectrum vectors in a 3-dimensional space (three is the number of analyzed bands). Smaller angles represent closer matches to the reference spectrum. We selected this method because it is relatively insensitive to topographic illumination and albedo effects (Kruse *et al.* 1993), which can be significant in the exposed intertidal zone. Figure 2 illustrates the steps of image processing: CIR image before and after removal of the areas not relevant to the analysis, after MNF transformation and after classification.

The conventional methodology of validation of classified remotely sensed images implies that all ground samples are unambiguously attributed to classes, but that was not the case in our study. We used a modified methodology that allowed us to estimate the accuracy of our classification by comparing the results of the classification with ground data from heterogeneous areas (i.e., the areas that did not have >90% of one type of cover). Each sample was attributed to a certain class not unambiguously, but in terms of probabilities, estimated from the percent cover values based on 100 points for ground samples and ca. 100 pixels at the corresponding area in the composite image. The elements of the classification error matrix were estimated by multiplication of these probabilities.

Validation of each image was conducted using a classification error matrix (also called confusion matrix or contingency table) and indices such as total accuracy (a percentage of correctly classified pixels),

Table 1. Number of samples with different cover types used as "training areas" and for validation during different surveys.

Date	Training Areas			Validation
	Ulva spp.	*Ceramium* spp.	Bare Surface (including mussels, mud, etc.)	
25-Jul-05	7	7	2	15
17-Sep-05	14	4	2	10
31-Oct-05	17	1*	2	6

* The sample contained 53% of *Ceramium* spp. and 47% of *Ulva* spp.

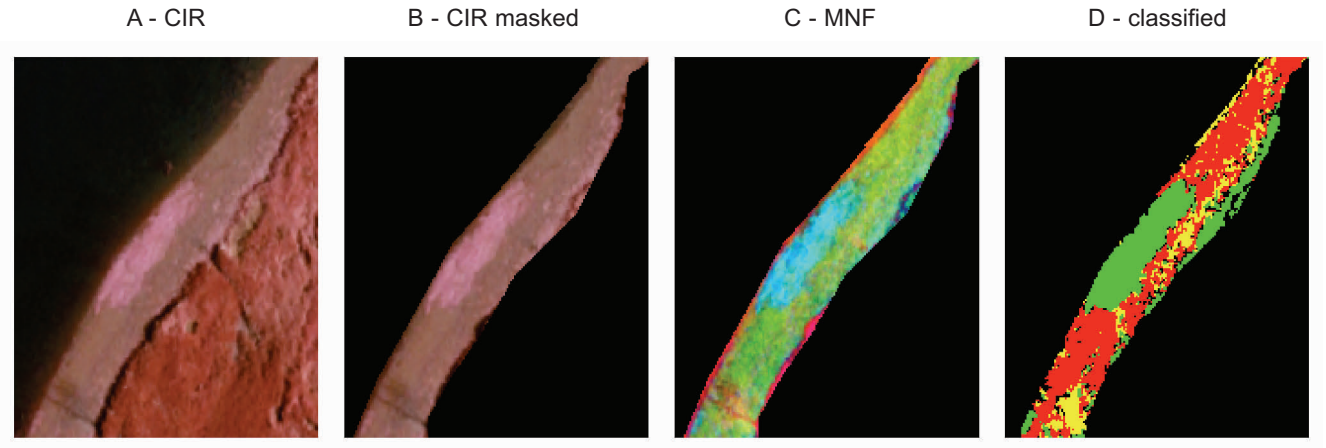

Figure 2. The subscene of CIR image (July 25, 2005) before (A) and after (B) removal of the areas not relevant to the analysis; the same image after MNF transformation (C) and after classification (D). Classes: *Ceramium* spp. (red); *Ulva* spp. (green); bare surface (yellow); unclassified (black).

producer accuracy (omission error), user accuracy (commission error), and KHAT statistic (Congalton and Green 1999, Lillesand and Kiefer 2000). KHAT is a statistical measure of the difference between the actual classification accuracy and the erroneous accuracy measure that could be obtained by completely random assignment of pixels to cover classes.

Based on previous studies showing longitudinal gradients in salinity, nutrient availability and macroalgal abundance in UNB (Kamer *et al.* 2001, RMA 2001, Kennison *et al.* 2003, Boyle *et al.* 2004), we divided UNB into four regions starting from the mouth of San Diego Creek and proceeding downstream toward the ocean (Regions A - D; Figure 1). Within each individual region, we determined the area of exposed intertidal mudflat covered by different classes as both an absolute number and as a percentage of the area exposed from the aerial images. We also calculated mean percent cover within each region from the ground-based data and compared the results to those from the image analysis. We did this for all of UNB as a whole as well.

The tidal levels during aerial surveys ranged from 5 cm (October 31), when almost all of the intertidal zone was exposed, to 60 and 70 cm (September 17 and July 25, respectively), when the lower stratum was covered with water. The percent coverage of different classes can be different in the different strata. As such, a correct method of comparison between the surveys would be to analyze only the upper stratum of the UNB intertidal zone, exposed during all three surveys. The exposed areas were very close during the surveys on September 17 and July 25. For the image taken on October 31, when the exposed area was substantially larger, we applied the water mask estimated for the survey when the tidal level was highest and the exposed intertidal zone was smallest (July 25). This was done for UNB as a whole and for each region separately (A - D).

Results

Aerial Imagery Classification

In the original CIR aerial images, the spectral characteristics of each cover type were very close (Figure 3). The brightness of the pixels within each sample varied over a wide range due to illumination and terrain effects, and the brightness of all three bands was strongly correlated within each class. The optical characteristics of identical classes also varied between different surveys, probably due to changes in illumination resulting from differences in sun angle and atmospheric conditions. In particular, on September 17 the brightness of all three bands was significantly lower than on July 25 and October 31. MNF transformation dramatically increased the contrast of all three images, resulting in better separability between the groups of samples. After MNF transformation, the brightness in different bands became uncorrelated, the clusters became more compact, and the differences among classes became more evident (Figure 3).

The results of cluster analysis show that image samples with similar spectral signatures that grouped out together actually represented different groups of ground data that were more like each other within groups than among. That shows that the method has

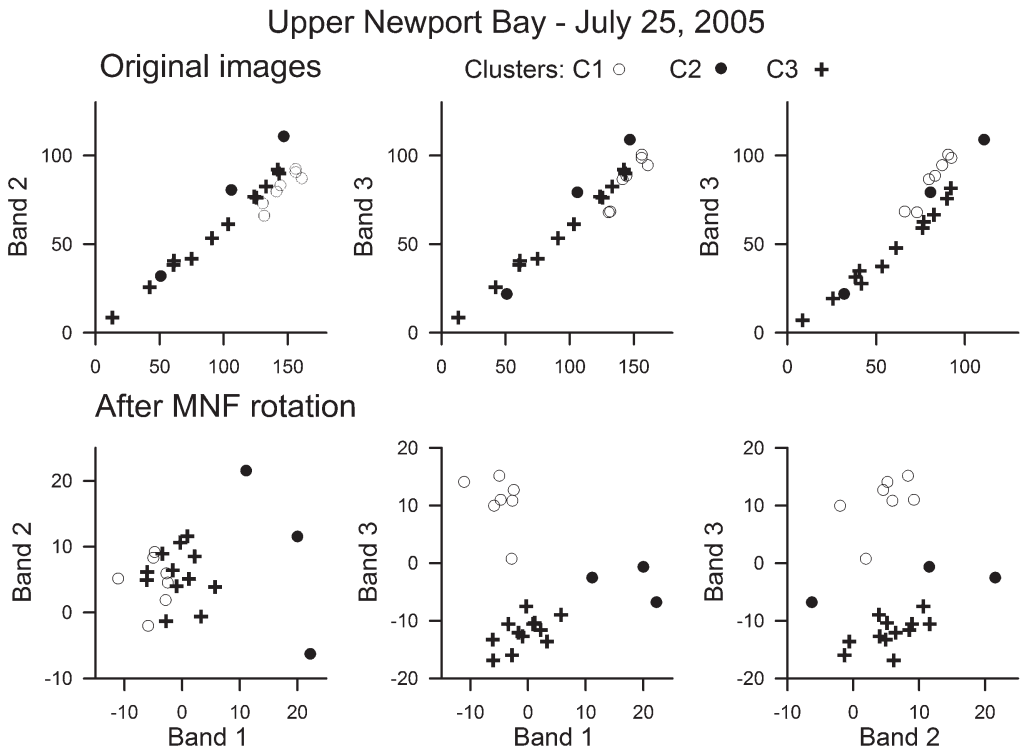

Figure 3. The locations of the means in the clusters of the Upper Newport Bay image taken July 25, 2005. Different symbols indicate clusters: *Ulva* spp. (C1); Bare surface (C2); and *Ceramium* spp (C3; Table 2). Above—original images (XY units are brightness); below—after Minimum Noise Fraction Rotation (XY units are dimensionless).

the ability to resolve among different types of cover relatively reliably (Table 2). The optimal number of clusters identified was three for July 25, four for September 17, and three for October 31. The differences between clusters were most evident in the July 25 images, when cluster C1 was almost exclusively *Ulva* spp., cluster C2 was 77% bare surface and cluster C3 was >90% *Ceramium* spp. Also, these three clusters were well distinguished on the images (Figure 3b). In the September 17 image, the differences between clusters were less evident, both in terms of percent cover (Table 2) and the optical properties of the clusters. Only one of the four clusters (C3) was almost exclusively *Ulva* spp.; cluster

Table 2. Number of samples and averaged macroalgal percent cover (mean ± standard error) in the clusters (C1 - C3 for July 25; C1 - C4 for September 17; C1 - C3 for October 31) classified on the basis of similarities of the spectral signatures of the samples.

Date	Cluster	Number of Samples	*Ulva* spp. %	*Ceramium* spp. %	Bare Surface %	Other (mussels, mud, etc.) %
25-Jul-05	C1	7	99.9 ±0.1	0.1 ±0.1	0.0 ±0.0	0.0 ±0.0
	C2	3	2.0 ±2.0	18.0 ±10.1	77.3 ±11.5	2.0 ±2.0
	C3	12	2.2 ±0.8	93.2 ±4.7	0.25 ±0.2	4.4 ±4.4
17-Sep-05	C1	8	72.0 ±11.8	27.3 ±12.0	0.8 ±0.5	0.0 ±0.0
	C2	3	23.0 ±15.3	0.0 ±0.0	15.7 ±15.7	61.3 ±30.8
	C3	11	99.4 ±0.4	0.0 ±0.0	0.6 ±0.4	0.1 ±0.1
	C4	8	28.4 ±11.1	71.6 ±11.1	0.0 ±0.0	0.0 ±0.0
31-Oct-05	C1	12	96.0 ±1.4	0.6 ±0.6	3.4 ±1.4	0.0 ±0.0
	C2	10	92.6 ±5.2	5.3 ±5.3	2.1 ±0.9	0.0 ±0.0
	C3	4	27.0 ±24.1	0.0 ±0.0	26.0 ±25.0	47.3 ±27.3

C4 was >70% *Ceramium* spp.; cluster C1 was a mixture of *Ulva* and *Ceramium* spp.; and cluster C2 was represented mostly by "other" cover types (e.g., mussel beds). Low separability between the clusters of ground samples in the September 17 images likely resulted from hazy atmosphere and low ambient brightness. In the October 31 image, the cluster dominated by bare mud and mussels was well separated from other stations while two clusters dominated by *Ulva* spp. were less distinguishable.

The accuracy of image classification was higher on July 25 and October 31 than on September 17 (Table 3). During July and October total classification accuracy was 85 - 88%. KHAT (i.e., the measure of statistical significance of total accuracy) was also high (0.65 - 0.74). The commission errors (i.e., the probabilities for each class to be contaminated by wrongly classified pixels) and omission errors (i.e., the probabilities for each class pixels to be wrongly classified) of both macroalgae classes did not exceed 15%. For bare surface, the omission and commission errors were higher: 30 - 33% in July and 22 - 28% in October. A tendency toward erroneous classification for unvegetated areas results from high variability of the optical properties of these surfaces, including rocks, mussel beds and other materials.

In September, low total accuracy (<40%) and KHAT (0.147) indicate that the results of classification have a relatively high level of uncertainty. Merging both macroalgae (*Ulva* spp. and *Ceramium* spp.) into one class substantially improved classification accuracy (Table 3). This suggests that under hazy conditions CIR photography could distinguish between macroalgae and bare surface but not between two types of macroalgae.

Macroalgal Coverage of Upper Newport Bay

Based on the analysis of aerial images, the exposed, intertidal mudflat area covered by macroalgae increased from July to October (Figures 4 and 5; Table 4). Coverage by *Ulva* spp. and *Ceramium* spp. combined was 37% in July, 57% in September, and 80% in October. In July, there was a longitudinal gradient in macroalgal abundance. Region D, closest to the ocean, had 19% macroalgal cover, which was mostly *Ceramium* spp. Region A, near the mouth of San Diego Creek, had 55% cover, which was mostly *Ulva* spp. (Figure 5; Table 4). In September, the cover of both *Ceramium* spp. and *Ulva* spp. increased in all regions of UNB. Combined cover of *Ceramium* spp. and *Ulva* spp. ranged from 37% in Region D to 79% in Region A. *Ulva* spp. was prolif-

Table 3. Accuracy of supervised classification for three surveys (July 25; September 17; and October 31). On September 17, the accuracy of classification was assessed for two macroalgal species (*Ulva* spp. and *Ceramium* spp.) separately and for macroalgae as a single cover type.

Date	Cover Type	Producer Accuracy (100% - omission error) %	User Accuracy (100% - commission error) %	Total Accuracy %	KHAT
25-Jul-05	*Ulva* spp.	99.5	86.3		
	Ceramium spp.	85.9	89.7		
	Bare surface, mussels, etc.	67.4	69.9		
				84.9	0.74
17-Sep-05	*Ulva* spp.	70.5	26.0		
	Ceramium spp.	54.5	47.3		
	Bare surface, mussels, etc.	10.7	47.0		
				38.2	0.15
17-Sep-05	Macroalgae	99.8	58.2		
	Bare surface, mussels, etc.	0.2	41.8		
				60.2	0.6
31-Oct-05	*Ulva* spp.	90.6	94.1		
	Ceramium spp.	0.0	0.0		
	Bare surface, mussels, etc.	78	71.7		
				88.0	0.65

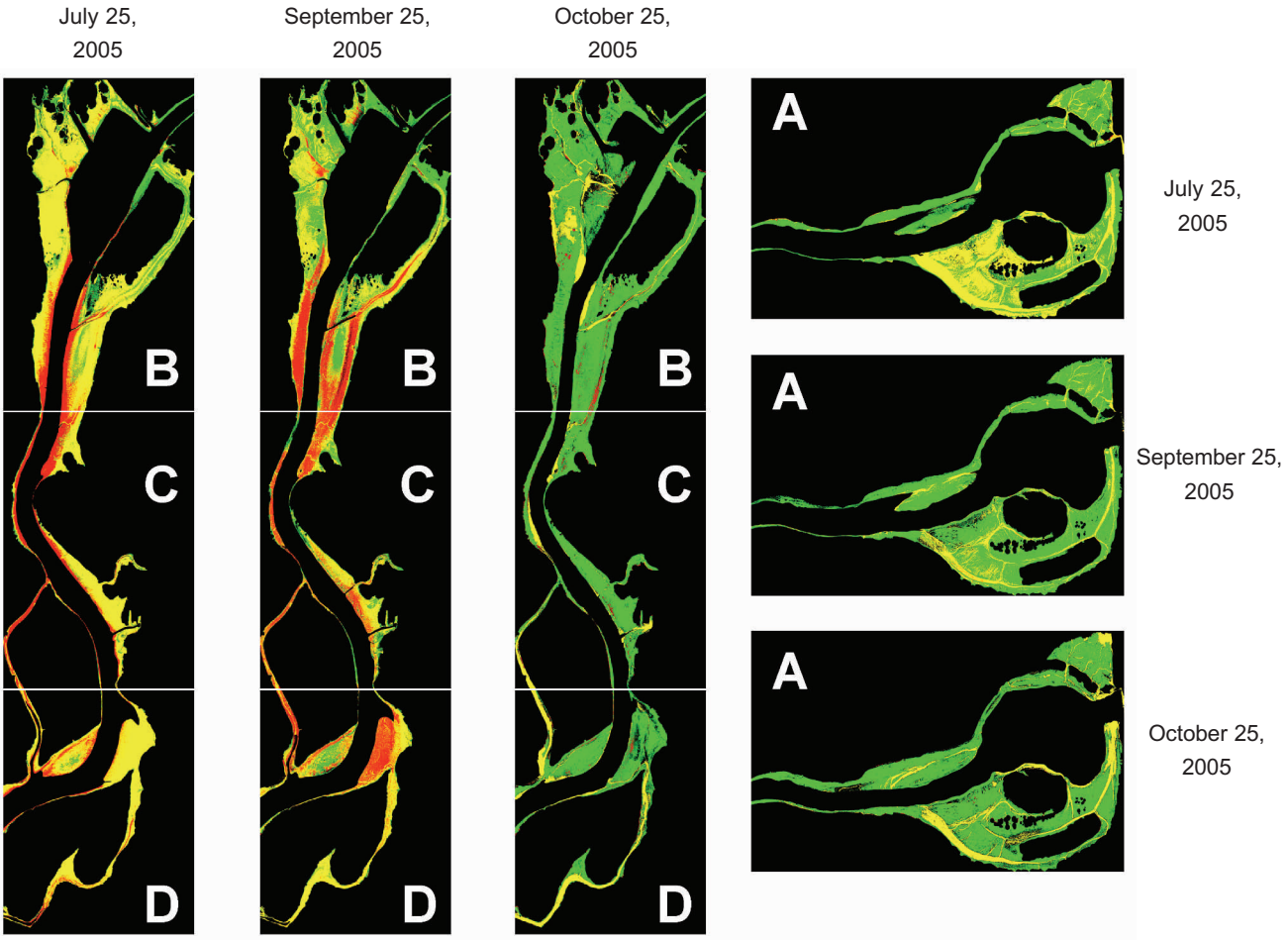

Figure 4. Spatial distribution of *Ulva* spp. (green), *Ceramium* spp. (red), and bare surface (yellow) in UNB on July 25, September 17, and October 31, 2005, estimated from CIR imagery classification. A, B, C, and D indicate different UNB regions (Figure 1).

ic throughout the estuary but *Ceramium* spp. was only found in the mid-estuary and downstream areas. The accuracy of September aerial survey was low however (see Table 3), and these results should be treated with caution. By the end of October, *Ulva* spp. coverage increased dramatically in all regions of UNB except Region A, where it had previously been high. *Ulva* spp. dominated in all UNB regions; *Ceramium* spp. was sparse, ranging from 0.5% to 4.2%. In September and October, the differences in macroalgae abundance between the upper and the lower parts of UNB were much less evident than in July.

Ground-based measurements of macroalgal abundance produced patterns similar to those based on aerial photographs, but the absolute values were different (Figure 5). Percent cover of macroalgae determined from aerial image analysis was often lower than that estimated from ground surveys. For example, in July much more *Ceramium* spp. was measured during ground surveys (51% cover) as compared to aerial surveys (13% cover). In the aerial images, 63% of the area was unvegetated, whereas ground data indicated that only 16% of the area was not covered by macroalgae. The remote sensing tended to detect more unvegetated area (i.e., the area that could not be identified as *Ceramium* spp. or *Ulva* spp.) than the ground surveys.

Discussion

Remote sensing via CIR aerial photography was a successful technique for mapping intertidal macroalgal distribution in UNB. The accuracy assessment indicated that the classifications generated from the aerial image analyses can be used with confidence, and estimates of algal cover from both ground-based measures and aerial photo-interpretation were generally comparable. The technique was most effective when macroalgal mats were dense. Similar work in Yaquina Bay in Oregon showed a

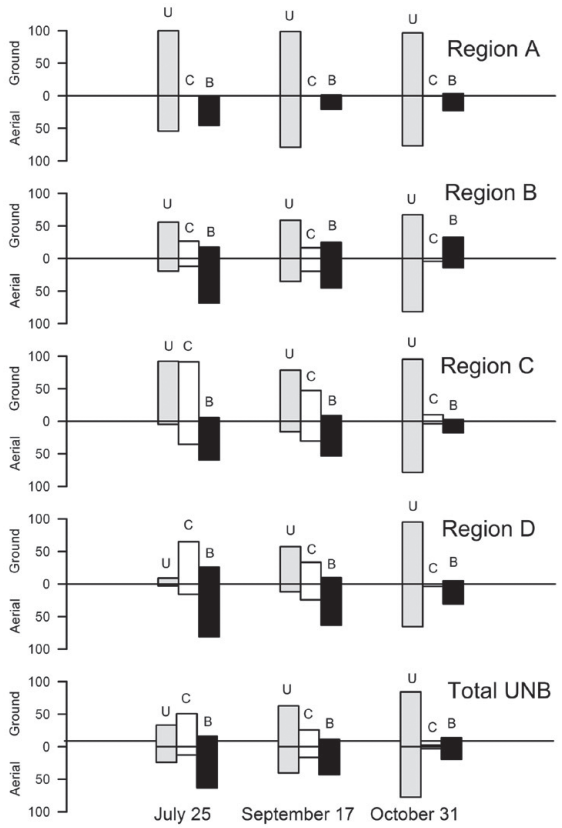

Figure 5. The percentages of ground samples (upper plots) and the areas of the Upper Newport Bay intertidal zone on aerial photography (lower plots) covered by *Ulva* spp. (U), *Ceramium* spp. (C), and other (mainly bare surface, B) in different UNB regions (A - D; Figure 1) and in the total Bay.

similar pattern of success. Good agreement between aerial image analysis and ground surveys in Yaquina Bay was found when vegetation exceeded 75% cover, but agreement decreased as the vegetation became less dense (D. Young, personal communication).

In our study, there were discrepancies between estimates of macroalgal cover from the aerial image analysis and the ground sampling, probably due to the fact that the macroalgae may have been more abundant along the water's edge where ground samples were collected than further across the mudflats; these latter areas could not reasonably be reached on foot. This pattern of distribution would have resulted in a ground data set that did not accurately represent the true distribution of macroalgae and bare surface within the system. We suspect that most of differences observed between the two data sets are due to an unintentional ground sampling bias toward vegetated areas. The end result is that data extrapolated from the ground samples likely overestimate macroalgal abundance. Estimates from aerial imagery are likely conservative because the methodology is less sensitive to small patches of algae compared to ground surveys, i.e., the quadrat method can measure tiny pieces of algae that the CIR will never resolve.

Spatial accuracy (i.e., the ability to precisely register the reference data) is a challenge in remotely sensed observations; it is especially true for aerial photography of macroalgae in intertidal zone, where collection of landmarks is a problem. All recognizable landmarks (e.g., water edge, creek beds, the patterns of vascular plants) in the UNB intertidal zone changed from one survey to another. To achieve high spatial accuracy, numerous landmarks should be collected in parallel with ground sampling; this process is time and labor consuming. In this study, the number of landmarks collected along the water's edge during ground sampling was ca. 25 (i.e., 2 - 3 per each aerial picture), and all these landmarks were used for georegistration rather than for spatial accuracy assessment. For spatial accuracy, numerous stable landmarks were obtained from the Google Earth website and used for both georegistration and spatial accuracy assessments, but these landmarks were located outside the intertidal zone, decreasing applicability of the spatial accuracy assessments in the area where samples were collected (i.e., along the water's edge). Because of potential incorrect spatial registration, some (unknown) portion of the image pixels associated with each sample could belong to a cover type different than what was measured on the ground, decreasing the accuracy of image classification. One way to overcome this problem is to sample only pixels whose identity is not influenced by potential registration errors, i.e., points located in broad homogenous areas at least several pixels away from field boundaries (Lillesand and Kiefer 2000). We suggest that most ground samples collected in UNB fit this condition. In each survey, at least 50 - 70% of the samples represented only one cover type, indicating that they were collected in homogenous areas. To test this assumption, we analyzed the homogeneity of the areas around the sampling sites by comparing the percentage of the cover types in the sample area of 100 pixels (2.5 x 2.5 m) size to a larger area of 400 pixels (5 x 5 m; Table 5). The results for small and large sample areas were very close (R^2 = 0.90 - 0.99), providing us with a reason to consider that even if the spectral characteristics of some sample sites were taken from the areas not

Table 4. Areas (ha and %) in the Upper Newport Bay covered by different cover types estimated from aerial photography.

Region	Cover Type	July 25	September 17	October 31	October 31 with Water Mask from July 25
A	*Ulva* spp.	8.6 (54.4%)	12.4 (79.0%)	12.6 (76.9%)	11.3 (77.1%)
	Ceramium spp.	0.04 (0.3%)	0.04 (0.3%)	0.1 (0.5%)	0.07 (0.5%)
	Bare surface, mussels, etc.	7.2 (45.3%)	3.2 (20.7%)	3.7 (22.6%)	3.3 (22.4%)
	Total	15.8 (100.0%)	15.7 (100.0%)	16.4 (100.0%)	14.7 (100.0%)
B	*Ulva* spp.	4.6 (19.3%)	9.5 (35.2%)	23.5 (81.8%)	19.9 (83.9%)
	Ceramium spp.	2.9 (12.2%)	4.7 (19.5%)	1.2 (4.2%)	1.0 (4.1%)
	Bare surface, mussels, etc.	16.5 (68.5%)	10.9 (45.3%)	4.0 (14.0%)	2.9 (12.0%)
	Total	24.1 (100.0%)	24.0 (100.0%)	28.7 (100.0%)	23.8 (100.0%)
C	*Ulva* spp.	0.4 (4.9%)	1.3 (16.2%)	7.2 (78.5%)	6.5 (83.5%)
	Ceramium spp.	2.9 (35.4%)	2.4 (30.5%)	0.4 (4.0%)	0.3 (4.5%)
	Bare surface, mussels, etc.	4.8 (59.7%)	4.2 (53.3%)	1.6 (17.5%)	0.9 (12.0%)
	Total	8.1 (100.0%)	7.9 (100.0%)	9.1 (100.0%)	7.8 (100.0%)
D	*Ulva* spp.	0.3 (2.7%)	1.2 (12.0%)	7.3 (65.7%)	6.3 (70.1%)
	Ceramium spp.	1.7 (16.0%)	2.5 (24.5%)	0.4 (3.6%)	0.4 (4.3%)
	Bare surface, mussels, etc.	8.5 (81.3%)	6.5 (63.5%)	3.4 (30.7%)	2.3 (25.6%)
	Total	10.4 (100.0%)	10.3 (100.0%)	11.1 (100.0%)	9.0 (100.0%)
Total UNB	*Ulva* spp.	13.9 (23.9%)	23.4 (40.4%)	50.6 (77.3%)	44.0 (79.7%)
	Ceramium spp.	7.5 (12.8%)	9.6 (16.6%)	2.1 (3.1%)	1.8 (3.2%)
	Bare surface, mussels, etc.	36.9 (63.3%)	24.9 (43.0%)	12.8 (19.5%)	9.4 (17.1%)
	Total	58.3 (100.0%)	57.9 (100.0%)	65.4 (100.0%)	55.2 (100.0%)

exactly corresponding to the location of ground sample, this displacement did not misrepresent the dominating cover type.

An accuracy of 85% is generally recommended as the threshold for acceptable results when mapping via remote sensing (Congalton and Green 1999). The total accuracy achieved in this study (60 - 88%) was close to this threshold and is comparable to accuracy achieved in other coastal habitat mapping efforts. Seagrass meadows in North Carolina were mapped with 72.6% accuracy (Ferguson and Korfmacher 1997) and benthic cover in Corsica was mapped with 62% to 92% accuracy (Pasqualini *et al.* 1997). Sheppard *et al.* (1995) achieved 91.3% accuracy when mapping shallow marine habitats at the Caribbean island Anguilla, and in Yaquina Bay, Orregon, accuracy >90% was achieved (D. Young, personal communication). It is hard to compare quantitatively the accuracy of remotely-sensed mapping in different studies where different methodology was used and different types of cover were assessed.

Table 5. Coefficients of determination (R^2) between the percentages of different cover types in samples of 100 pixels (2.5 x 2.5 m) and 400 pixels (5 x 5 m).

Date	*Ulva* spp.	*Ceramium* spp.	Bare Surface
25-Jul	0.994	0.989	0.987
17-Sep	0.97	0.954	0.91
31-Oct	0.903	0.99	0.9

The degree of accuracy achieved in mapping ground cover based on remotely-sensed imagery depends on proper selection of the method of image processing. This study illustrates that the MNF method (Green *et al.* 1988) is an effective tool to remove noise and enhance the differences between the cover types used for classification and validation of classification results. MNF transformation is based on the Principle Component Analysis (PCA) method, different modifications of which

have been repeatedly used for analysis of remotely sensed imagery, including aerial photography of benthic habitats (Ferguson and Korfmacher 1997; Pasqualini *et al.* 1997, 1998). A salient feature of this method is a decrease of the number of bands, making this method especially useful for processing of hyperspectral imagery, where the number of bands often exceeds 100. Even when the number of bands was as small as three as in our study, MNF transformation significantly enhanced the image contrast, resulting in better classification.

The SAM method of assessing similarity between pixels is recommended for the analysis of images in which brightness is highly variable but strongly correlated between bands, which can result presumably from terrain effects. The SAM method estimates similarity from the angles between the pixel vectors in multidimensional space, which corresponds to the ratio between the brightness values of different bands rather than the absolute brightness values. It should be noted that MNF transform removes a significant portion of correlation between bands, enabling usage of other methods of classification. In our study, the SAM method was also applied to original CIR images before MNF transform and provided satisfactory results, though they were not as good as the results obtained after MNF transform.

The accuracy of our assessment could have been improved if we had taken a slightly different approach to the image classification. If we had targeted the placement of the ground samples so that they were attributed unambiguously to homogenous samples representing different cover types, it would have increased the number of samples available for use as training areas. This would have allowed a slightly higher accuracy in the image classification. This would have been consistent with the approach recommended by Lillesand and Kiefer (2000), who suggest that when the image is highly mosaic (as was the case in this study), relatively large (i.e., significantly exceeding the accuracy of georegistration) homogenous areas covered by each cover type (i.e., training areas) should be selected. The cover types with optical properties that are expected to vary (e.g., bare surface) should be sampled in greater frequency than the cover types of more consistent color (e.g., macroalgae). It is worth mentioning that the minimum number of samples recommended by Congalton and Green (1999), 50 for each class, was not achievable in this study because we prioritized completion of the ground survey within one tidal cycle, thus limiting the time available to collect ground samples.

The observed spatial pattern of macroalgal distribution is typical of UNB. Previous studies also showed very high cover of *Ulva* spp. at the head of UNB and the highest *Ceramium* spp. cover at the seaward end. Macroalgal abundance is often strongly related to nutrient availability (Sfriso *et al.* 1987, Hernandez *et al.* 1997, Schramm 1999). Kennison *et al.* (2003), Boyle *et al.* (2004), and Sutula *et al.* (2006) each measured higher water column dissolved nitrogen (N) and phosphorus (P) concentrations at the head of UNB compared to further downstream, which in part could explain the persistent, high density of *Ulva* spp. in Region A. Region A also typically has the highest sediment N and P concentrations and benthic nutrient efflux (Kennison *et al.* 2003, Sutula *et al.* 2006).

One limitation of CIR aerial photography in assessing macroalgae for the purposes of eutrophication assessment is that it can only quantify the spatial extent of algal mats and not the thickness. Only percent cover, not biomass, can be determined. Previous studies (Kamer *et al.* 2001, Kennison *et al.* 2003) have not attempted to correlate macroalgal percent cover and biomass, and we do not recommend doing so at this time either. A statistically significant, reliable relationship is unlikely because the thickness of algal mats can vary greatly (K. Kamer, personal observations). However, percent cover provides a reasonable metric for abundance and clearly depicts temporal and spatial changes in macroalgae. Different remote sensing technologies, such as hyperspectral imagery, which collects data in many bands in the visible and near-infrared spectra, may provide the ability to discriminate between mats of different thicknesses, but this has yet to be investigated.

Another limitation is that CIR photography can only be used to assess the distribution of exposed vegetation, rather than submerged vegetation. When benthic plants are covered by water, even at shallow depths, their optical signatures are dramatically obscured (Sheppard *et al.* 1995) and CIR often does not resolve between submerged vegetation and other cover types because water strongly absorbs near-infrared radiance. To successfully use CIR aerial photography to map intertidal vegetation, the lowest tide possible should be targeted in order to maximize exposure of the emergent intertidal zone. Natural color photographs have been successfully used for visualization of submerged vegetation (Ferguson *et*

al. 1993, Marshall and Lee 1994, Pasqualini *et al.* 2001), and hyperspectral imaging may offer unique advantages for mapping subtidal vegetation as well (Dierssen *et al.* 2003). These studies were conducted in relatively clear waters. It is unknown whether or not any type of imagery could penetrate UNB's turbid waters.

We further recommend collecting all images during similar tidal phases since the amount of intertidal area exposed depends on tidal level. In southern California the tidal range can be as much as 2 m, and the collection of aerial imagery at different tidal heights resulted in different exposure of intertidal mudflat areas (Table 6). While we normalized our data to the total area surveyed by calculating each classification as a percentage of the whole, we were concerned that differences in macroalgal distribution with elevation affect our results. It is also necessary to collect ground data for each individual aerial survey because the spectral signatures of the cover types were not transportable through time. The illumination conditions of each survey varied with sun angle and azimuth and atmospheric conditions. This caused the same class of cover, such as *Ulva* spp., to produce different spectra in the aerial images for each survey.

CIR photography is an effective tool for synoptically assessing estuarine, intertidal macroalgal coverage. The ability to evaluate an entire system at once offers distinct advantages over ground-based sampling in terms of both accuracy and effort. The spatial extent of the macroalgae measured in this study can be used as a baseline for comparison with future studies to assess changes over time. This technology can also be used to assess relative eutrophication synoptically in multiple systems and to assess regional patterns and trends. Hyperspectral imaging and high resolution satellite imagery should also be explored in the future with the following considerations in mind: spatial resolution, ability to resolve macroalgal mat thickness, ability to target tidal phase, and cost.

Literature Cited

Ahern, J., J. Lyons, J. McClelland and I. Valiela. 1995. Invertebrate response to nutrient-induced changes in macrophyte assemblages in Waquoit Bay. *Biological Bulletin* 189:241-242.

Andrefouet, S., C. Payri, E.J. Hochberg, L.M. Che and M.J. Atkinson. 2003. Airborne hyperspectral detection of microbial mat pigmentation in Rangiroa atoll (French Polynesia). *Limnology and Oceanography* 48:426-430.

Andrefouet, S., C. Payri, E.J. Hochberg, C. Hu, M.J. Atkinson and F.E. Muller-Karger. 2004. Use of in situ and airborne reflectance for scaling-up spectral discrimination of coral reef macroalgae from species to communities. *Marine Ecology - Progress Series* 283:161-177.

Table 6. The areas of the Upper Newport Bay intertidal zone (m^2) during different surveys and the environmental conditions including tidal phase and solar angle and azimuth.

Survey	Region	Intertidal Zone Area (ha)	Intertidal Zone Exposed (%)	Time of Survey	Tidal Level (m)	Solar Elevation Angle	Solar Azimuth
25-Jul-05	A	15.8	96.30%				
	B	24.1	84.00%	10:25-10:45 a.m.	0.7	66°	57°
	C	8.1	89.00%				
	D	10.4	93.70%				
	Total	58.3	89.10%				
17-Sep-05	A	15.7	95.70%				
	B	24	83.60%	1:15-1:35 p.m.	0.6	53°	-35°
	C	7.9	86.80%				
	D	10.3	92.80%				
	Total	57.9	88.50%				
31-Oct-05	A	16.4	100%				
	B	28.7	100%	2:00-2:30 p.m.	0.05	32°	-39°
	C	9.1	100%				
	D	11.1	100%				
	Total	65.4	100%				

Avery, T.E. and G.L. Berlin. 1992. Fundamentals of Remote Sensing and Airphoto Interpretation. Prentice Hall. Upper Saddle River, NJ.

Boyer, K.E. 2002. Linking community assemblages and ecosystem processes in temperate and tropical coastal habitats. Unpublished Ph.D. thesis, University of California, Los Angeles. Los Angeles, CA.

Boyle, K.A., K. Kamer and P. Fong. 2004. Spatial and temporal patterns in sediment and water column nutrients in a eutrophic southern California estuary. *Estuaries* 27:378-388.

Bulthuis, D.A. 1995. Distribution of seagrasses in a North Puget Sound estuary: Padilla Bay, Washington, USA. *Aquatic Botany* 50:99-105.

Caloz, R. and C. Collet. 1997. Geographic information systems (GIS) and remote sensing in aquatic botany: methodological aspects. *Aquatic Botany* 58:209-228.

Campbell, J.B. 1987. Introduction to Remote Sensing. Guilford Press. New York, NY.

Carder, K.L., R.G. Steward, R.F. Chen, S.K. Hawes, A. Lee and C.O. Davis. 1993. AVRIS calibration and application in coastal oceanic environments: tracers of soluble and particulate constituents in the Tampa Bay coastal plume. *Photogrammetric Engineering and Remote Sensing* 59:339-344.

Congalton, R.G. and K. Green. 1999. Assessing the Accuracy of Remotely Sensed Data: Principles and Practices. Lewis Publishers. Boca Raton, FL.

Deysher, L.E. 1993. Evaluation of remote-sensing techniques for monitoring giant kelp populations. *Hydrobiologia* 261:307-312.

Dierssen, H.M., R.C. Zimmerman, R.A. Leathers, T.V. Downes and C.O. Davis. 2003. Ocean color remote sensing of seagrass and bathymetry in the Bahamas Banks by high-resolution airborne imagery. *Limnology and Oceanography* 48:444-455.

Ferguson, R.L. and K. Korfmacher. 1997. Remote sensing and GIS analysis of seagrass meadows in North Carolina, USA. *Aquatic Botany* 58:241-258.

Ferguson, R.L., L.L. Wood and D.B. Graham. 1993. Monitoring spatial change in seagrass habitat with aerial photography. *Photogrammetric Engineering and Remote Sensing* 59:1033-1038.

Gerstenberg, G. 1989. Management Plan Upper Newport Bay Ecological Reserve. State of California Resource Agency, Department of Fish and Game. Newport Beach, CA.

Green, A.A., M. Berman, P. Switzer and M.D. Craig. 1988. A transformation for ordering multispectral data in terms of image quality with implications for noise removal. *IEEE Transactions on Geoscience and Remote Sensing* 26:65-74.

Harding, L.W., Jr., E.C. Itsweir and W.E. Esaias. 1994. Estimation of phytoplankton biomass in the Chesapeake Bay from aircraft remote sensing of chlorophyll concentrations, 1989-92. *Remote Sensing of Environment* 49:41-56.

Hayden, H.S., J. Blomster, C.A. Maggs, P.C. Silva, M.J. Stanhope and J.R. Waaland. 2003. Linnaeus was right all along: *Ulva* and *Enteromorpha* are not distinct genera. *European Journal of Phycology* 38:277-294.

Hayden, H.S. and J.R. Waaland. 2002. Phylogenetic systematics of the Ulvaceae (Ulvales, Ulvophyceae) using chloroplast and nuclear DNA sequences. *Journal of Phycology* 38:1200-1212.

Hernandez, I., G. Peralta, J.L. Perez-Llorens, J.J. Vergara and F.X. Niell. 1997. Biomass and dynamics of growth of *Ulva* species in Palmones River estuary. *Journal of Phycology* 33:764-772.

Hilton, J. 1984. Airborne remote sensing for freshwater and estuarine monitoring. *Water Research* 18:1195-1223.

Hoogenboom, H.J., A.G. Dekker and J.F. De Haa. 1998. Retrieval of chlorophyll and suspended matter in inland waters from CASI data by matrix inversion. *Canadian Journal of Remote Sensing* 24:144-152.

Jensen, J.R. 2000. Remote Sensing of the Environment: an Earth Resource Perspective. Prentice Hall. Upper Saddle River, NJ.

Jensen, J.R., J.E. Estes and L. Tinney. 1980. Remote sensing techniques for kelp surveys. *Photogrammetric Engineering and Remote Sensing* 46:743-755.

Kamer, K., K.A. Boyle and P. Fong. 2001. Macroalgal bloom dynamics in a highly eutrophic southern California estuary. *Estuaries* 24:623-635.

Kendrick, G.A., B.J. Hegge, A. Wyllie, A. Davidson and D.A. Lord. 2000. Changes in seagrass cover on Success and Parmelia Banks, Western Australia between 1965 and 1995. *Estuarine, Coastal and Shelf Science* 50:341-353.

Kennison, R.L., K. Kamer and P. Fong. 2003. Nutrient dynamics and macroalgal blooms: a comparison of five southern California estuaries. Technical Report 416. Southern California Coastal Water Research Project. Westminster, CA.

Kirkman, H. 1996. Baseline and monitoring methods for seagrass meadows. *Journal of Environmental Management* 47:191-201.

Kruse, F.A., A.B. Lefkoff, J.B. Boardman, K.B. Heidebrecht, A.T. Shapiro, P.J. Barloon and A.F.H. Goetz. 1993. The Spectral Image Processing System (SIPS) - Interactive Visualization and Analysis of Imaging spectrometer Data. *Remote Sensing of Environment* 44:145-153.

Kwak, T.J. and J.B. Zedler. 1997. Food web analysis of southern California coastal wetlands using multiple stable isotopes. *Oecologia* (Berlin) 110:262-277.

Lehmann, A. and J.-B. Lachavanne. 1997. Geographic information systems and remote sensing in aquatic botany. *Aquatic Botany* 58:195-207.

Lillesand, T.M. and R.W. Kiefer. 2000. Remote sensing and image interpretation (4th ed.). John Wiley & Sons. New York, NY.

Malthus, T.J. and D.G. George. 1997. Airborne remote sensing of macrophytes in Cefni Reservoir, Anglesey, UK. *Aquatic Botany* 58:317-332.

Marshall, T.R. and P.F. Lee. 1994. Mapping aquatic macrophytes through digital image analysis of aerial photographs: an assessment. *Journal of Aquatic Plant Management* 32:61-66.

Mumby, P.J., E.P. Green, C.D. Clark and A.J. Edwards. 1998. Digital analysis of multispectral airborne imagery of coral reefs. *Coral Reefs* 17:59-69.

Mumby, P.J., J.D. Hedley, J.R.M. Chisholm, C.D. Clark, H. Ripley and J. Jaubert. 2004. The cover of living and dead corals from airborne remote sensing. *Coral Reefs* 23:171-183.

Myers, J.S. and R.L. Miller. 2005. Optical airborne remote sensing. pp. 51-67 *in*: R. . Miller , C. . Del Castillo and B. . McKee (eds.), Remote Sensing of Coastal Aquatic Environments. Technologies, Techniques and Applications. Springer. Dordrecht.

Nixon, S.W. 1995. Coastal marine eutrophication: A definition, social causes, and future concerns. *Ophelia* 41:199-219.

Paerl, H.W. 1999. Cultural eutrophication of shallow coastal waters: coupling changing anthropogenic nutrient inputs to regional management approaches. *Limnologica* 29:249-254.

Pasqualini, V., C. Pergent-Martini, P. Clabaut, H. Marteel and G. Pergent. 2001. Integration of aerial remote sensing, photogrammetry, and GIS technologies in seagrass mapping. *Photogrammetric Engineering and Remote Sensing* 67:99-105.

Pasqualini, V., C. Pergent-Martini, P. Clabaut and G. Pergent. 1998. Mapping of *Posidonia oceanica* using aerial photographs and side scan sonar: application off the Island of Corsica (France). *Estuarine, Coastal and Shelf Science* 47:359-367.

Pasqualini, V., C. Pergent-Martini, C. Fernandez and G. Pergent. 1997. The use of airborne remote sensing for benthic cartography: advantages and reliability. *International Journal of Remote Sensing* 18:1167-1177.

Peckol, P. and J.S. Rivers. 1995. Physiological responses of the opportunistic macroalgae *Cladophora vagabunda* (L.) van den Hoek and *Gracilaria tikvahiae* (McLachlan) to environmental disturbances associated with eutrophication. *Journal of Experimental Marine Biology and Ecology* 190:1-16.

Pregnall, A.M. and P.P. Rudy. 1985. Contribution of green macroalgal mats (*Enteromorpha* spp.) to seasonal production in an estuary. *Marine Ecology - Progress Series* 24:167-176.

Raffaelli, D., P. Balls, S. Way, I.J. Patterson, S. Hohmann and N. Corp. 1999. Major long-term changes in the ecology of the Ythan estuary, Aberdeenshire, Scotland: How important are physical factors? *Aquatic Conservation: Marine and Freshwater Ecosystems* 9:219-236.

Raffaelli, D., J. Limia, S. Hull and S. Pont. 1991. Interactions between the amphipod *Corophium volu-*

tator and macroalgal mats on estuarine mudflats. *Journal of the Marine Biological Association of the United Kingdom* 71:899-908.

Richardson, L.L., D. Buison, C.J. Lui and V. Ambrosia. 1994. The detection of algal photosynthetic accessory pigments using Airborne Visible-Infrared Imaging Spectrometer (AVRIS) spectral data. *Marine Technology Society Journal* 28:10-21.

RMA. 2000. Newport Bay residence time study. Prepared for the Irvine Company. Resource Management Associates Inc. Suisun City, CA.

RMA. 2001. Newport Bay Water Quality Model Development 3-D Stratified Flow Analysis. Prepared for California State Water Resources Control Board. Resource Management Associates Inc. Suisun City, CA.

Robbins, B.D. 1997. Quantifying temporal change in seagrass areal coverage: the use of GIS and low resolution aerial photography. *Aquatic Botany* 58:259-267.

Schramm, W. 1999. Factors influencing seaweed responses to eutrophication: Some results from EU-project EUMAC. *Journal of Applied Phycology* 11:69-78.

Schramm, W. and P.H. Nienhuis (eds.). 1996. Marine Benthic Vegetation: Recent Changes and the Effects of Eutrophication. Springer-Verlag. New York, NY.

Sfriso, A., A. Marcomini and B. Pavoni. 1987. Relationships between macroalgal biomass and nutrient concentrations in a hypertrophic area of the Venice Lagoon. *Marine Environmental Research* 22:297-312.

Sfriso, A., B. Pavoni, A. Marcomini and A.A. Orio. 1992. Macroalgae, nutrient cycles, and pollutants in the Lagoon of Venice. *Estuaries* 15:517-528.

Sheppard, C.R.C., K. Matheson, J.C. Bythell, P. Murphy, C. Blair Myers and B. Blake. 1995. Habitat mapping in the Caribbean for management and conservation: use and assessment of aerial photography. *Aquatic Conservation: Marine and Freshwater Ecosystems* 5:277-298.

Sutula, M., K. Kamer, J. Cable, H. Collis, W.M. Berelson and J. Mendez. 2006. Sediments as an internal source of nutrients to Upper Newport Bay, California. Technical Report 482. Southern California Coastal Water Research Project. Westminster, CA.

Thiel, M. and L. Watling. 1998. Effects of green algal mats on infaunal colonization of a New England mud flat - long-lasting but highly localized effects. *Hydrobiologia* 375/376:177-189.

Vahtmae, E., T. Kutser, G. Martin and J. Kotta. 2006. Feasibility of hyperspectral remote sensing for mapping benthic macroalgal cover in turbid coastal waters - a Baltic Sea case study. *Remote Sensing of Environment* 101:342-351.

Valiela, I., K. Foreman, M. LaMontagne, D. Hersh, J. Costa, P. Peckol, B. DeMeo-Andreson, C. D'Avanzo, M. Babione, C.H. Sham, J. Brawley and K. Lajtha. 1992. Couplings of watersheds and coastal waters sources and consequences of nutrient enrichment in Waquoit Bay Massachusetts. *Estuaries* 15:443-457.

Ward, D.H., C.J. Markon and D.C. Douglas. 1997. Distribution and stability of eelgrass beds at Izembek Lagoon, Alaska. *Aquatic Botany* 58:229-240.

Werdell, P.J. and C.S. Roesler. 2003. Remote assessment of benthic substrate composition in shallow waters using multispectral reflectance. *Limnology and Oceanography* 48:557-567.

Wilkie, D.S. and J.T. Finn. 1996. Remote sensing imagery for natural resources monitoring: a guide for first-time users. Columbia University Press. New York, NY.

Young, D.R., D.T. Specht, P.J. Clinton and H.I. Lee. 1998. Use of color infrared aerial photography to map distributions of eelgrass and green macroalgae in a non-urbanized estuary of the Pacific northwest USA. Paper presented at the Fifth International Conference on Remote Sensing for Marine and Coastal Environments.

Acknowledgements

This work was funded by the California State Water Resources Control Board through a grant to the County of Orange Resources and Development Management Department (SWRCB Agreement No. 04-192-558-0). The authors thank Doug Shibberu at the Santa Ana Regional Water Quality Control Board, George Edwards and Amanda Carr at the

County of Orange, and Jim Hyde at Irvine Ranch Water District for project support. Thanks also to David R. Young at the US Environmental Protection Agency, Western Ecology Division, for technical expertise and guidance; Andy Aguilar, Emily Briscoe, Michelle Cordrey, Liesl Tiefenthaler, and Dawn Petschauer for their assistance in the field, often very early in the morning. The authors also express appreciation for three anonymous reviewers who provided helpful comments and input.